Soils and Foundations 2015;55(5):951–962

HOSTED BY

ELSEVIER

The Japanese Geotechnical Society

Soils and Foundations

www.sciencedirect.com
journal homepage: www.elsevier.com/locate/sandf

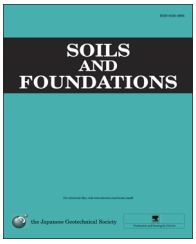

Bender element tests in dry and saturated sand: Signal interpretation and result comparison

Xiaoqiang Gu[a,1], Jun Yang[b,*], Maosong Huang[a], Guangyun Gao[a]

[a]Department of Geotechnical Engineering and Key Laboratory of Geotechnical and Underground Engineering of the Ministry of Education, Tongji University, Shanghai, China

[b]Department of Civil Engineering, The University of Hong Kong, Pokfulam, Hong Kong, China

Received 30 June 2014; received in revised form 5 March 2015; accepted 5 June 2015
Available online 26 September 2015

Abstract

The shear wave (S-wave) velocities in dry and saturated sand specimens at various confining pressures and densities were measured by bender elements (BE) incorporated in a resonant column (RC) apparatus with the cyclic torsional shear (TS) function. The received BE signals were analyzed by different interpretation methods, including the start–start method, the peak–peak method, the cross correlation method and the cross power method. Parametric studies on several scenarios of input and output wave forms were also carried out to examine the reliability of the different interpretation methods and the underlying reasons for the discrepancies. The results obtained from the BE, RC and TS tests were compared carefully. They showed that, for BE tests on saturated sand specimens, the effective density accounting for the wave dispersion effect should be used to convert the measured S-wave velocity into small strain shear modulus G_0, whereas, for RC tests, the conventional saturated density should be used. It was also found that under the same void ratio and confining pressure, the G_0 value of saturated sand is about 7–10% lower than that for dry sand, and that the effect of the sample preparation method is coupled with the test method in the evaluation of the G_0 values.

Keywords: Sand; Laboratory test; Bender element; Resonant column; Torsional shear; Shear modulus; Saturation; Sample preparation method

1. Introduction

It is well recognized that soil behavior is generally nonlinear and plastic in nature. However, at strain levels below 0.001%, the response of soil is usually assumed to be elastic and the corresponding shear modulus is referred to as the small strain shear modulus (G_0) or the maximum shear modulus. The small strain shear modulus of soil plays an important role in many geotechnical designs, such as machine foundations, earthquake ground-response analyzes and liquefaction potential evaluations (e.g., Richart et al., 1970; Andrus and Stokoe, 2000; Yang and Yan, 2009).

Several techniques have been developed in the geotechnical profession for measuring G_0, including the resonant column test (Hardin and Richart, 1963; Stokoe et al., 1995), the quasi-static loading test with high resolution strain measurements (Kokusho, 1980; Hoque and Tatsuoka, 1998; Ezaoui and Di Benedetto, 2009) and the bender element test (Dyvik and Madshus, 1985; Viggiani and Atkinson, 1995; Brignoli et al., 1996). In the resonant column (RC) test, a cylindrical soil specimen is subjected to a torsional excitation and the resonant frequency is found by varying the excitation frequency. Given resonant frequency f_n, shear wave (S-wave) velocity V_s and

*Corresponding author.
E-mail address: junyang@hku.hk (J. Yang).
[1]Formerly from The University of Hong Kong.
Peer review under responsibility of The Japanese Geotechnical Society.

http://dx.doi.org/10.1016/j.sandf.2015.09.002

associated G_0 can be calculated by

$$V_s = \frac{2\pi f_n L}{\beta} \tag{1}$$

and

$$G_0 = \rho (V_s)^2 \tag{2}$$

where ρ is the mass density involved in the wave propagation, L is the length of the specimen and β is a parameter that can be determined by

$$\beta \tan \beta = \frac{I}{I_0} \tag{3}$$

where I is the mass polar moment of inertia of the specimen and I_0 is the mass polar moment of inertia of the components above the specimen.

In a quasi-static loading test (e.g., torsional shear and triaxial tests), the shear strain of soil subjected to a small shear stress increment (i.e., the resulting shear strain is at a small strain level) is directly measured with high resolution transducers and the G_0 value of the soil is calculated based on the stress–strain curve.

Ever since it was introduced to geotechnical applications by Shirley and Hampton (1978), the bender element (BE) test has been increasingly incorporated into laboratory testing devices to measure the V_s of soils due to its simplicity and cost-effectiveness. In a BE test, by monitoring the input and output signals, V_s can be directly calculated as follows:

$$V_s = \frac{L_{tt}}{\Delta t} \tag{4}$$

where L_{tt} is the wave travel distance, which usually takes the tip-to-tip distance between the source and the receiving elements, and Δt is the wave travel time. Given the V_s, the G_0 value can be evaluated by Eq. (2).

One of the main concerns with the above test methods is whether these methods can provide consistent G_0 values. Youn et al. (2008) showed that the G_0 values of clean sand measured from BE, RC and TS tests were consistent with each other. Ferreira et al. (2006) and Camacho-Tauta et al. (2014) reported that the G_0 values of Porto granitic residual soil and kaolinite from RC and BE generally agreed with each other. However, Souto et al. (1994) reported that the consistency of the G_0 values measured from BE and RC depended on the grading of the soil. In addition, the signal interpretation for determining the shear wave travel time in BE tests remains a tricky problem and different interpretation methods may give different results (Greening and Nash, 2004; Viana da Fonseca et al., 2009; Yamashita et al., 2009; Yang and Gu, 2013). The discrepancy between BE and RC measurements is usually attributed to the uncertainty of the signal interpretation in the BE tests. However, the questions as to which signal interpretation method gives the most reliable results and what causes the discrepancies among the different methods have not been fully solved.

One more concern is the dispersion (i.e., frequency dependency) of the S-wave velocity in saturated soil (Biot, 1956) because different testing methods use significantly different frequencies. The frequency usually lies in the range of several tenths to several Hz in quasi-static loading tests and several tens Hz in RC tests, but several to a few tens kHz in BE tests. Youn et al. (2008) showed that instead of the saturated density, an effective density which accounts for the wave dispersion effect should be used to convert the measured V_s to G_0 in BE tests on clean sand. Otherwise, the G_0 value would be remarkably overestimated. According to Biot's theory (Biot, 1956), the effective density is equal to the saturated density in soils with low permeability, such as clays and silts, and it is less than the saturated density in soils with high permeability, such as clean sands and gravels (Yang and Sato, 1998; Qiu and Fox, 2008). In summarizing the results of international parallel tests conducted to evaluate the G_0 of Toyoura sand by BE tests, Yamashita et al. (2009) reported that G_0 values were not notably affected by the saturation conditions. It is to be noted, however, that the saturated density was used in Yamashita et al. (2009) to convert the measured V_s to G_0. Nakagawa et al. (1997) showed that the measured V_s under saturated conditions was smaller than the one predicted using Biot's theory with the same G_0 value under dry conditions, meaning that the decrease in G_0 values under saturated conditions is likely to be due to the wetting of the contacts between the soil particles. Hence, it is necessary to investigate the effect of both the S-wave dispersion and the saturation.

In the study of soil properties, reconstituted specimens are usually used in laboratory tests due to the difficulty of obtaining undisturbed specimens. The effect of the sample preparation method (SPM) on the cyclic loading behavior of sand at large levels of strain and liquefaction resistance has recently been well studied (see Sze and Yang, 2014 and the references therein). However, the effect of the sample preparation method on G_0 has not been as well addressed. For example, Tatsuoka et al. (1979) performed RC and TS tests on Toyoura sand specimens reconstituted by various preparation methods (e.g., dry tamping (DT), rodding, air pluviation, moist tamping and saturated vibration). They concluded that the shear modulus was insensitive to the sample preparation method for a wide range in strain amplitudes. On the contrary, Rashidian et al. (1995) measured the S-wave velocity of Toyoura sand specimens prepared by the air pluviation (AP), water sedimentation (WS) and moist tamping (MT) methods, using accelerometers attached to the membrane, and showed that the effect of SPM seemed to depend on the void ratio (Fig. 1(a)). It is noted that at a void ratio of 0.72, the G_0 values of the specimens by the MT and WS methods were around 70% higher than those prepared by the AP method, but that they were quite close to each other when the void ratio was larger than 0.87. By employing BE tests, however, De Alba et al. (1984) showed that the G_0 values of the clean uniform sand specimens prepared by the MT method were about 20% higher than those prepared by the AP method at all tested void ratios, as shown in Fig. 1(b). These observations indicate that the effect of SPM may depend on the test method, and thus, further study is needed to clarify this issue.

This paper presents a comprehensive testing program conducted on Toyoura sand specimens at various effective confining pressures and densities under both dry and saturated conditions. The G_0 values of specimens reconstituted by

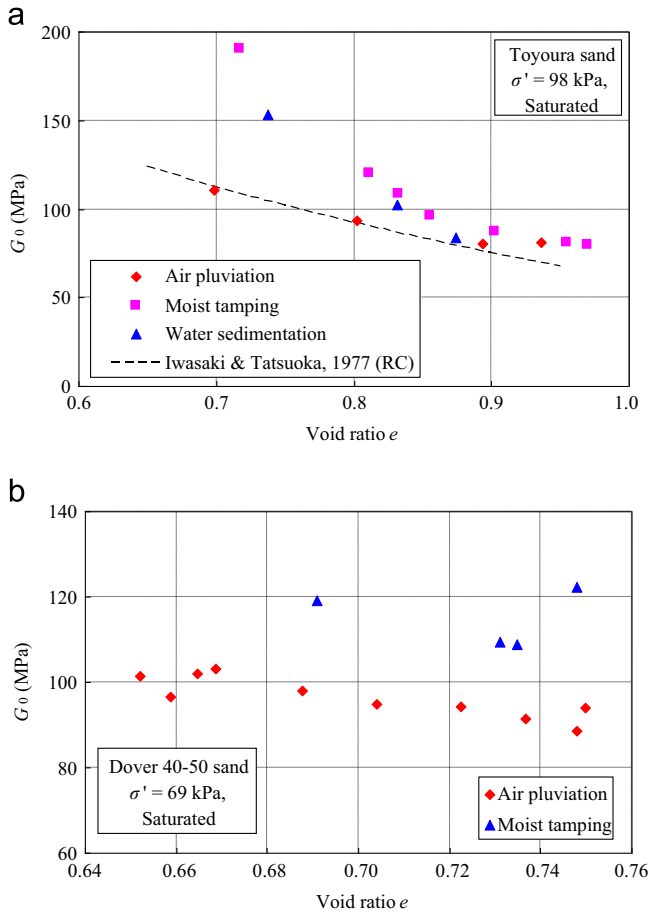

Fig. 1. Effect of sample preparation method on G_0 values observed in the literature: (a) Rashidian et al., 1995 and (b) De Alba et al., 1984.

different methods were measured by BE, RC and TS tests. For the BE tests, the signals were analyzed using different interpretation methods, and a parametric study was conducted to investigate the underlying reasons for the observed discrepancies yielded from the different interpretation methods. In the present paper, the G_0 values of sand specimens under dry and saturated conditions, obtained from the BE, RC and TS tests, are compared. The potential coupling effects of the test method, the saturation conditions and the sample preparation method on the G_0 of clean sand are investigated.

2. Test apparatus, material and procedure

2.1. Test apparatus

The apparatus used in this study is a standard RC incorporating the BE and cyclic TS functions, as schematically shown in Fig. 2. The RC is of a bottom-fixed and top-free configuration. It can accommodate a soil specimen 50 mm in diameter and 100 mm in height. The uniqueness of this test apparatus lies in that BE, RC and TS tests can be simultaneously performed on identical specimens, which can certainly improve the reliability of the test results.

Each bender element is 11 mm in width and 1.2 mm in thickness, with a penetration depth of 2.0 mm. Unlike the conventional design, the BE is able to generate not only shear waves, but also compression waves (i.e., P-wave) by modifying the wiring configuration (Lings and Greening, 2001; Gu et al., 2013). The system delay has been determined to be 5.5 μs by calibration tests with the element tips in direct contact. The calibration also indicates that the initial polarizations of the input and output signals are the same. Special attention should be paid to such an initial polarization relation as it will change in the S-wave test once one element (usually the element on the top cap) rotates 180° toward the other.

In the TS tests, the specimen is subjected to a small cyclic toque, generated by the coil–magnet system, and the shear stress is calculated from this torque. The angle of twist of the specimen is measured by a proximeter (see Fig. 2); and thus, the shear strain can be determined. Based on the stress–strain curve, the G_0 value can be evaluated. The shear strain amplitude lies in the range of 0.0005–0.0008% by controlling the input voltage to the coil.

2.2. Test material and sample preparation

Toyoura sand was used in the test program. It is clean and uniform silica sand with sub-rounded to sub-angular particles. Table 1 lists the main properties of Toyoura sand. The G_0 values of Toyoura sand have been extensively studied in the literature, which facilitates the evaluation of the reliability of the TS, RC and BE tests in this study.

Given the importance of sample preparation methods on the sand behavior (e.g., Sze and Yang, 2014), three typical sample preparation methods, including dry tamping (DT), air pluviation (AP) and moist tamping (MT), were adopted to reconstitute the specimens for testing. The details of each preparation method are introduced in the following:

(1) *Dry tamping*: The sample was prepared with 5 layers. For each layer, an amount of oven-dried soil, based on the desired void ratio, was slowly deposited into the split mold with no fall height by a glass funnel with a nozzle having a diameter of 6.5 mm. Then, the soil layer was carefully leveled by a ruler and compacted to the desired height with a bronze tamper. Before the construction of the next layer, the surface was carefully scarped to enhance the connection between the two layers. Specimens prepared by DT were tested under both dry and saturated conditions.

(2) *Air pluviation*: This sample was also prepared with 5 layers. For each layer, the amount of oven-dried soil, based on the desired void ratio, was transferred to a glass funnel with a nozzle having a diameter of 3.0 mm. Then, sand was pluviated into the split mold at a constant falling height to the sand layer surface. During the pluviation, the funnel was moved around the sand surface and lifted slowly to keep a constant falling height. Different void ratios were achieved by adjusting the falling height.

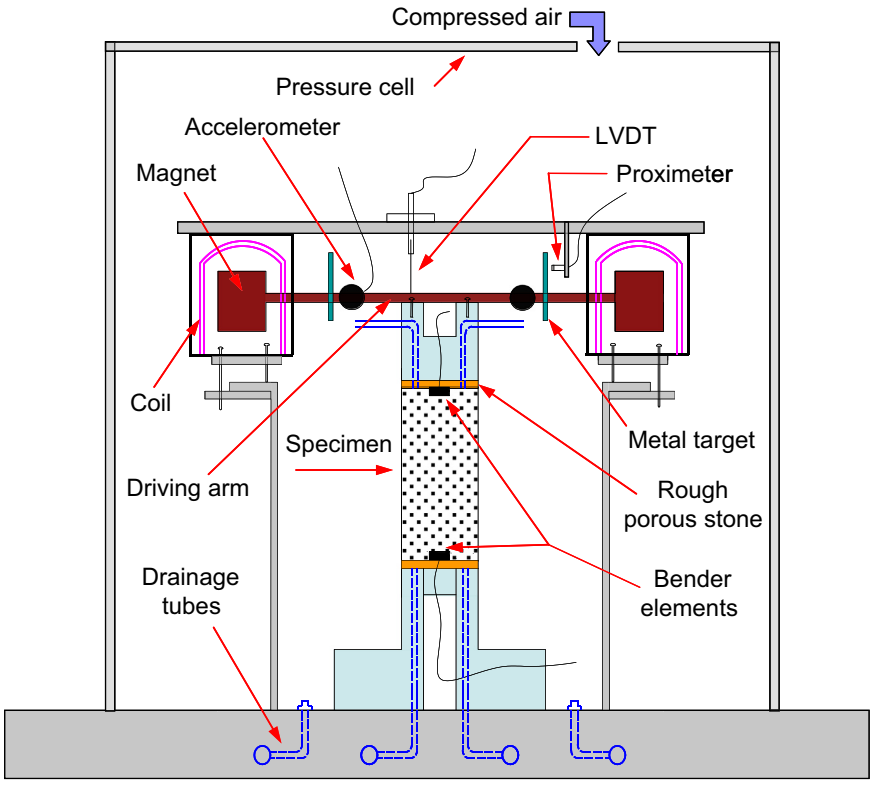

Fig. 2. Schematic illustration of the resonant column apparatus with bender elements used in the study (not to scale).

Table 1
Fitting results for G_0 measurements for specimens prepared by different methods.

SPM	Test condition	Test method	Fitting results		
			$F(e)$	A	n
DT	Dry	BE	$(2.17-e)^2/(1+e)$	95.4	0.41
		RC		92.4	0.41
		TS		92.0	0.41
DT	Saturated	BE with ρ_{sat}		96.3	0.45
		BE with ρ_{Biot}		83.8	0.45
		RC		85.9	0.40
		TS		84.6	0.40
AP	Saturated	BE with ρ_{Biot}		86.5	0.45
		RC		86.3	0.40
		TS		87.4	0.39
MT	Saturated	BE with ρ_{Biot}		104.6	0.40
		RC		92.2	0.40
		TS		91.1	0.39

(3) *Moist tamping*: Sand with a 5% moisture content was prepared by mixing oven-dried sand and water. The moist sand was put in a sealed container for one night to make the moisture uniform. The sample construction was the same as that for the DT method. Compared to the DT method, however, much greater compaction energy was required to achieve the same desired void ratio by the MT method due to the capillary force induced by the moisture. All the specimens prepared by the MT method were tested under saturated conditions in order to eliminate the capillary effect occurring under such moist conditions.

2.3. Test procedure

After the sample preparation, a suction of 25 kPa was applied to stand the specimen. Then, the dimensions of the specimen were measured and the initial void ratio was determined. For tests under saturated conditions, the specimen was flushed with CO_2 and then with de-aired water. Back pressure was applied to ensure the saturation of the specimen.

In each test, an isotropic effective confining pressure was applied in four steps, namely, 50, 100, 200 and 400 kPa. During the consolidation, the axial deformation and the change in volume of the specimen under saturated conditions were measured by an LVDT and a GDS controller, respectively. Thus, the specimen dimensions and the void ratio can be updated at each stress stage. Note that only the axial deformation was measured under dry conditions and that the void ratio was updated assuming isotropic deformation.

3. Results under dry conditions

3.1. Signal interpretation

Despite its increasing popularity, the determination of travel time Δt in BE tests remains a tricky problem involving subjectivity and uncertainty. This is due primarily to the near field effect and signal distortions. Various interpretation methods, including the start–start (S–S) method, the peak–peak (P–P) method, the cross correlation (CC) method and the cross power (CP) method, have been proposed to determine

the travel time (Viggiani and Atkinson, 1995; Greening and Nash, 2004; Lee and Santamarina, 2005; Viana da Fonseca et al., 2009). However, different methods usually yield different results, and there seem to be no firm conclusions about which method gives the most reliable results. Generally, it is expected that BE tests will provide similar G_0 values to those from RC tests. If not, the discrepancy is usually believed to be induced by the signal interpretation method. Hence, the received BE signals under different conditions are analyzed in detail in this paper.

Fig. 3 shows the received S-wave signals for a dry DT specimen by one cycle of sinusoidal input at different frequencies. The specimen was isotropically confined at a pressure of 100 kPa and a void ratio of 0.798. To evaluate the performances, different signal interpretation methods were used to analyze the signals, and the results are shown in Fig. 4, together with the results from the RC tests (at a shear strain level of 6.9×10^{-6}). In Fig. 4, S–S1 and S–S2 mean the results obtained from the start-to-start method by taking points S1 (indicated by the upward triangle in Fig. 3) and S2 (indicated by the X) as the first arrival; P-P1 and P-P2 mean the results obtained from the peak-to-peak method by taking peak points P1 and P2 in Fig. 3 as the first arrival, respectively; and CC-1 and CC-2 mean the results obtained from the cross correlation method by taking the 1st and 2nd peaks in the cross correlation spectrum, respectively. Details of these methods and analyzes can be found in Yang and Gu (2013) and Gu (2012). It can be seen that different interpretation methods provide significantly different results. The S–S method generally provides the most stable results at different input frequencies. Other methods significantly overestimate the G_0 value at low input frequencies and underestimate the G_0 value at high input frequencies. Observing the characteristics of the output signals and taking the results obtained from the RC tests as a reference, it is reasonable to deduce that the first arrival of the S-wave is around the dashed line (or the upward triangle) in Fig. 3. For consistency, the S–S method with the first arrival, indicated by the upward triangle at 10 kHz, was used to determine the travel time in the study. Note that the amplitude of the wave form, corresponding to the first arrival, is much smaller than the succeeding ones.

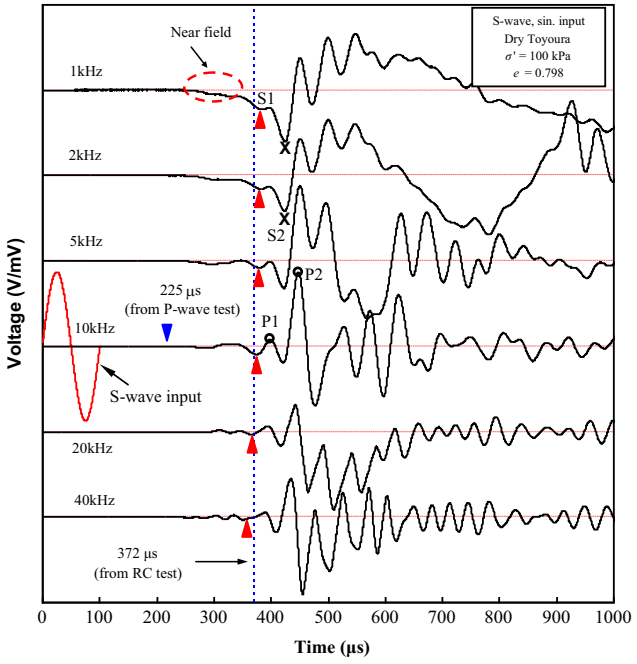

Fig. 3. Received S-wave signals in a dry DT specimen.

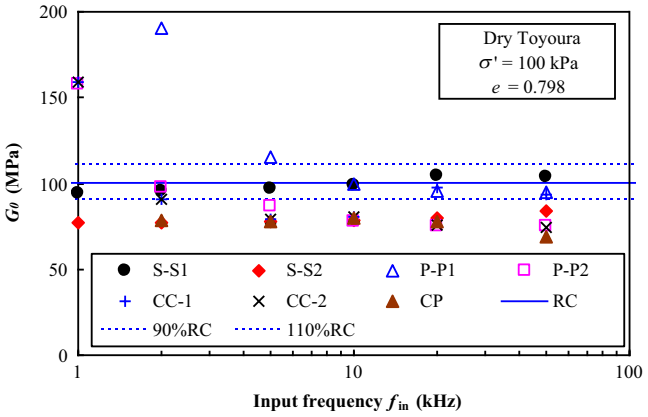

Fig. 4. G_0 values obtained by different interpretation methods in a BE test.

3.2. Parametric study

As seen above, different interpretation methods provide significantly different results for the same signals, depending on the input frequency. To investigate the underlying reasons for the observed discrepancies, a parametric study has been performed on two conceptual models (denoted as m_1 and m_2), as shown in Fig. 5. In model m_1, both input and output signals are single sinusoidal pulses and input frequency f_{in} is fixed at 10 kHz, while output frequency f_{out} varies from 4 kHz to 20 kHz to represent the frequency distortion. In model m_2, to simulate the reverberation in the experiments, the output signal is a sinusoidal wave of two cycles at 10 kHz, while the input signal is the same as in model m_1. The amplitudes of the two wave cycles are A_1 and A_2, respectively, and the larger one is assumed to be unity. The actual travel time is assumed to be 200 μs and the actual G_0 is denoted as G_0^{ref}.

Fig. 6 plots the normalized shear modulus G_0/G_0^{ref} for model m_1 as a function of f_{out}/f_{in}. It is seen that the S–S method gives correct G_0 values at all output frequencies, but other methods give correct G_0 values only at $f_{out}=f_{in}$. The P–P, CC and CP methods will underestimate or overestimate G_0 when f_{out} is lower or higher than f_{in}, respectively, but the degree of error by the P–P method is less significant than the degrees of error by the CC and CP methods. Meanwhile, the CC and CP methods yield identical results.

For a better illustration, the case of an input of 10 kHz and an output of 5 kHz for model m_1 is examined, and the CC and CP spectra are shown in Fig. 7. Evidently, a unique peak exists in the CC spectrum and the corresponding travel time is easily determined to be 250 μs. On the other hand, there are several discrete portions in the phase-frequency diagram (Fig. 7c),

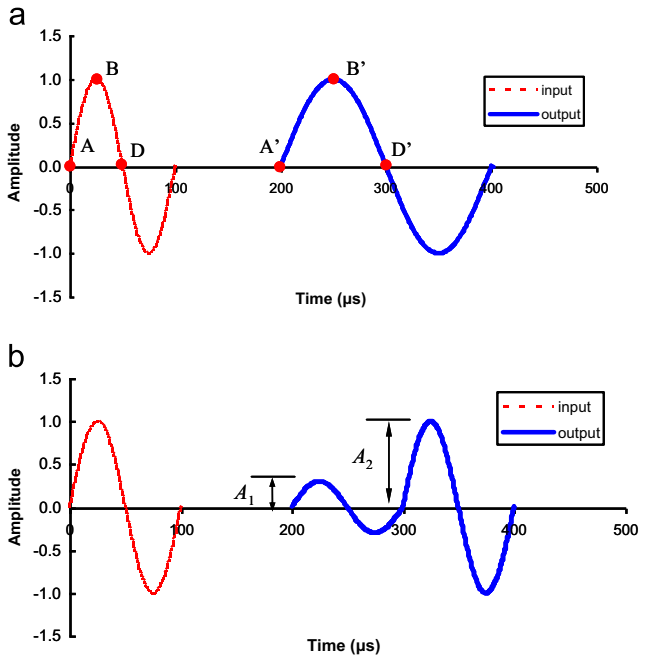

Fig. 5. Illustrations of (a) model m_1 and (b) model m_2 in the parametric study.

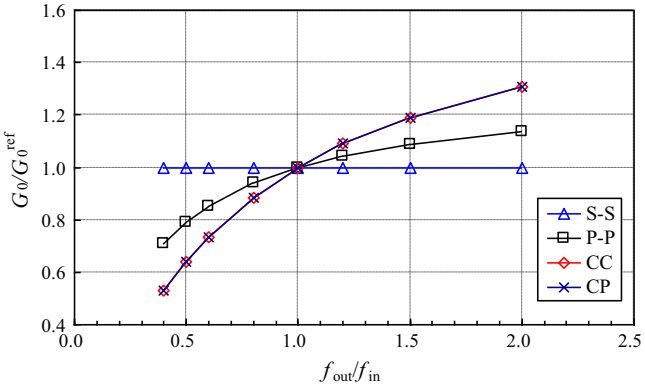

Fig. 6. Results of model m_1 in the parametric study.

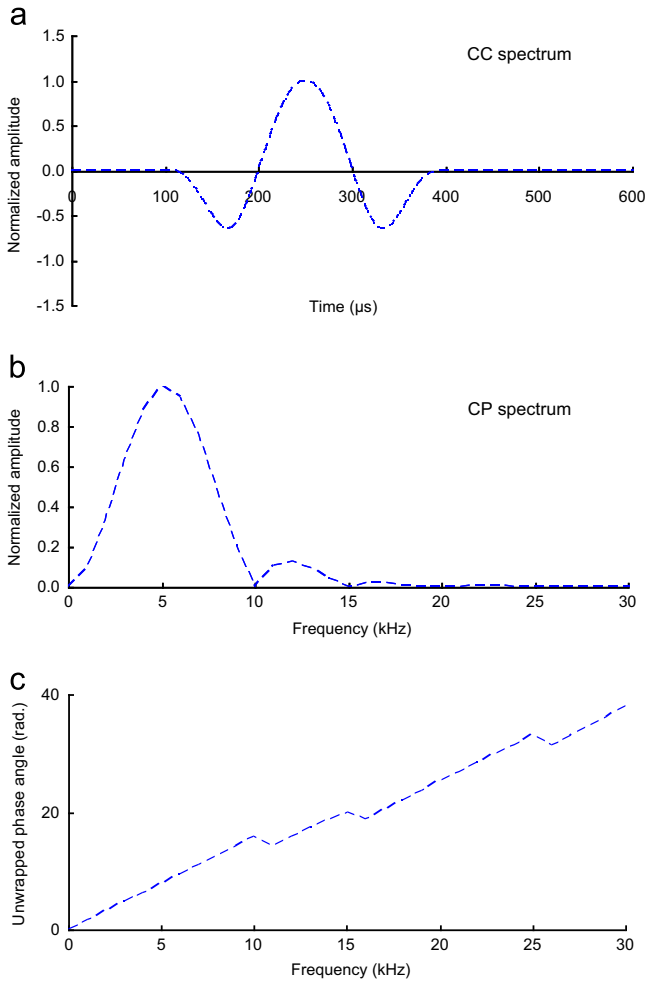

Fig. 7. Results for model m_1 with $f_{in}=10$ kHz and $f_{out}=5$ kHz: (a) CC spectrum, (b) CP spectrum and (c) unwrapped phase angle.

although each portion is linear with an identical slope. It is interesting to note that the intersections of different portions correspond to zero points in the CP spectrum (Fig. 7b). Here, as suggested by Yamashita et al. (2009), the frequency range for which the amplitude of the CP spectrum is the largest (i.e., 1–10 kHz) is used, and the travel time is determined to be 250 μs. Further analysis shows that the travel time increases by $0.25(1/f_{out}-1/f_{in})$ in the P–P method and $0.5(1/f_{out}-1/f_{in})$ in the CC and CP methods. Actually, the travel time determined by the CC and CP methods corresponds to the time interval between point D in the input signal and point D′ in the output signal (see Fig. 5). The above analysis indicates that the difference in frequency between the input and output signals may induce discrepancies among the different interpretation methods.

Fig. 8 shows the results of model m_2. It is interesting to observe that the S–S, P–P1 and CC-1 methods always give correct values. The P–P2 and CC-2 methods, however, give considerately lower values, as the travel time corresponds to the second cycle of the output. It is consistent with the observation that the CC method, corresponding to the first peak in the CC spectrum, provides more reasonable results (Yamashita et al., 2009), rather than the maximum peak as in the definition of the CC method. The more interesting observation shows the results obtained when using the CP method. The CP spectra and the unwrapped phase angle-frequency diagrams are shown in Fig. 9, together with the frequency range used to calculate the travel time. As seen in Fig. 9, when A_1/A_2 is less than 0.5, the CP method yields similar results to the P–P2 and CC-2 methods; they significantly underestimate the G_0 values. In other words, if the amplitude of the first arrival is less than half of the second one, the travel time by the CP method is the travel time corresponding to the second wave cycle. As A_1/A_2 increases, the G_0 value determined with the CP method increases. When A_1/A_2 is larger than 2.0, the CP method generally gives the correct value, and the influence of the second cycle is negligible.

To provide a better explanation, the case of $A_1/A_2=0.8$ is analyzed in detail and the CC and CP spectra are shown in Fig. 10. It is clear that two peaks exist in the CC spectrum and

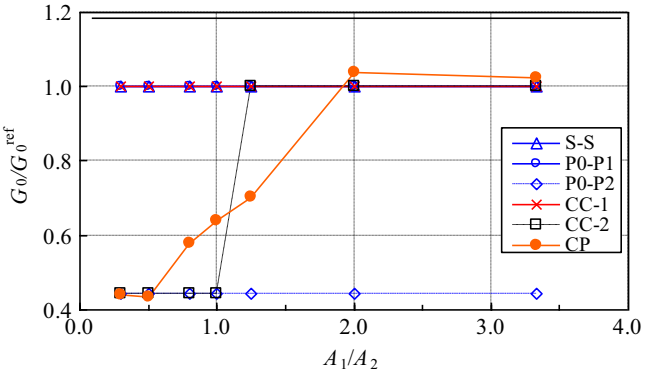

Fig. 8. Results for model m_1 in the parametric study.

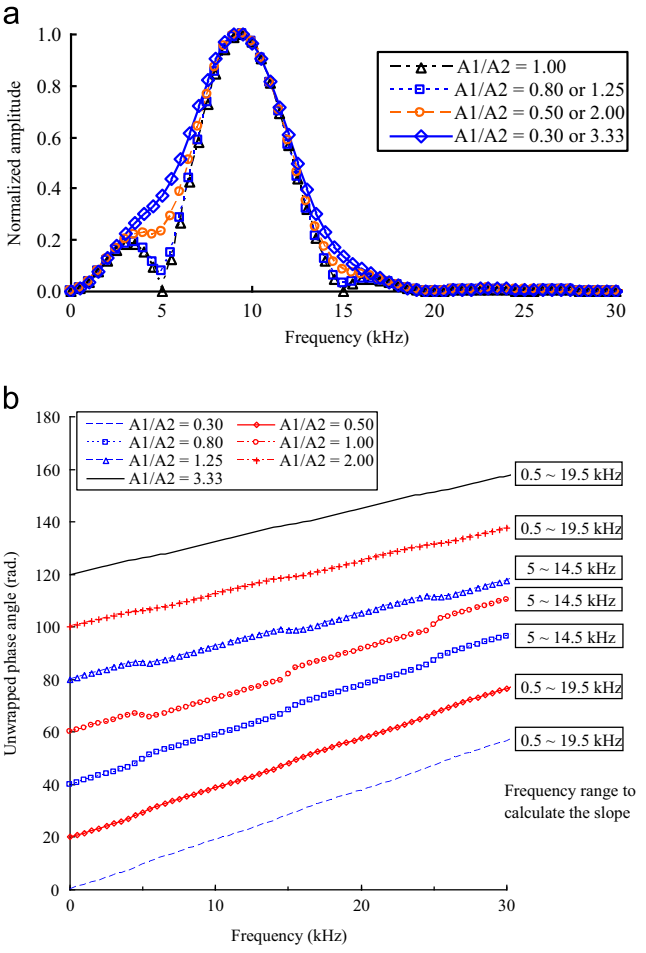

Fig. 9. (a) CP spectrum and (b) unwrapped phase angle for model m_2 in the parametric study.

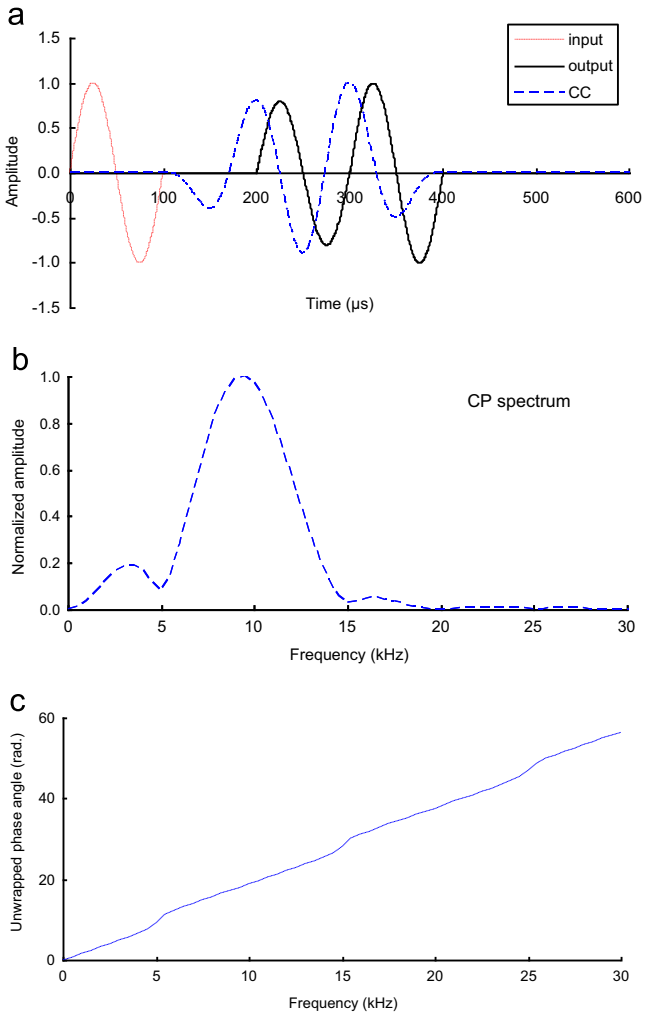

Fig. 10. Results of the case with $A_1/A_2=0.8$ in model m_2: (a) CC spectrum, (b) CP spectrum and (c) unwrapped phase angle.

that they correspond to the arrival of the two wave cycles. Based on the CP spectrum in Fig. 10(b), the frequency range of 5.5–14.5 kHz is used in the CP method and the calculated travel time is 263 μs, which is much larger than the correct value of 200 μs. It seems that the wave cycle with the largest amplitude (i.e., the power) in the output signal plays a dominant role in determining the travel time in the CP method, while other wave cycles affect the results, and the degree of the effect depends on their amplitudes. As seen in Fig. 9(b), the nonlinearity in the phase angle-frequency diagram increases when A_1/A_2 approaches 1.0, indicating the increasing influence of the other cycle. When $A_1/A_2=1.0$, the travel time obtained by the CP method is 250 μs, which is the average value of the travel times of the first and second wave cycles. These results explain why the CP method usually provides much lower values than the S–S method in the literature; the reasons are that the output signal has multiple wave cycles and the amplitude of the wave cycle corresponding to the first arrival is not the largest one (e.g., Greening and Nash, 2004; Viana da Fonseca et al., 2009).

3.3. Comparison of results from BE, RC and TS tests

To evaluate the reliability of the signal interpretation as well as the testing system, the G_0 values for Toyoura sand specimens at different void ratios and confining pressures, obtained from the BE tests based on the S–S1 method, are compared with those from the RC and TS tests and with the data collected from the literature, as shown in Fig. 11. Note that the strain amplitudes in the RC and TS tests are less than

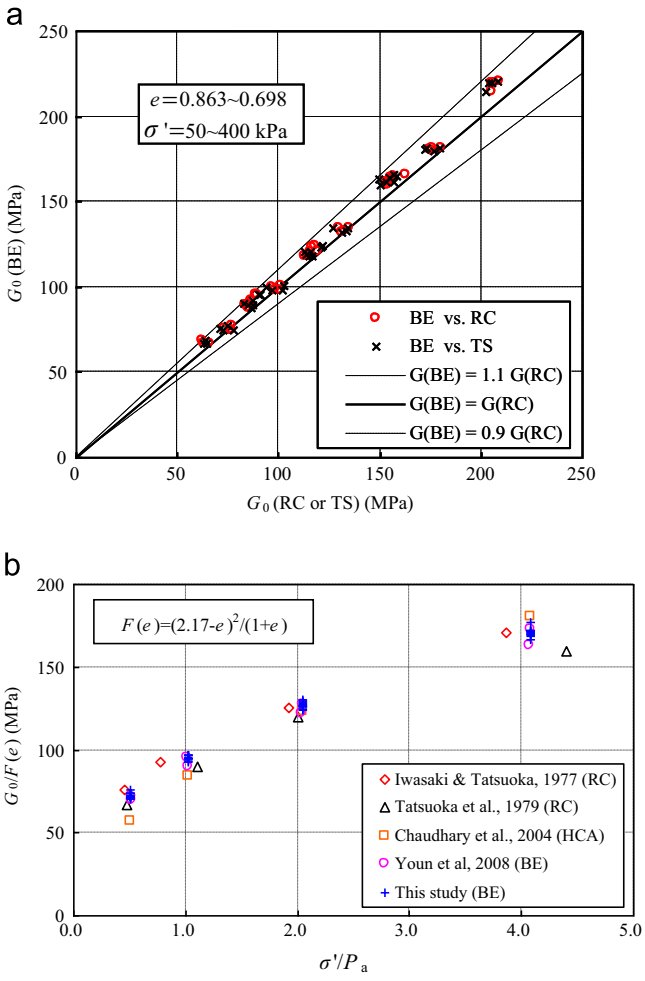

Fig. 11. Comparison of G_0 values of Toyoura sand obtained by BE tests with (a) RC test data and (b) test data in the literature.

8×10^{-6}. The G_0 values from the BE tests are slightly higher than those from the RC and TS tests, especially at high confining pressures. Possible reasons for this difference may be that (a) the strain level in the BE tests is somehow lower than that in the RC and TS tests and (b) the RC and TS tests measure the overall stiffness of the specimen, whereas the BE test measures the local stiffness of the wave travel path which tends to be stiffer than the whole specimen. Generally, the G_0 values for Toyoura sand from the BE, RC and TS tests in this study agree well with those in the literature. This suggests that the effect of frequency on the small strain stiffness of dry sand is negligible, which is consistent with the test results by Kim et al. (1991) and Youn et al. (2008).

4. Results under saturated conditions

4.1. Signal interpretation

Fig. 12 shows the received S-wave signals in a saturated DT specimen at the same effective confining pressure and void ratio as the dry specimen discussed previously. Compared with the dry specimen, it seems to be easier to determine the first

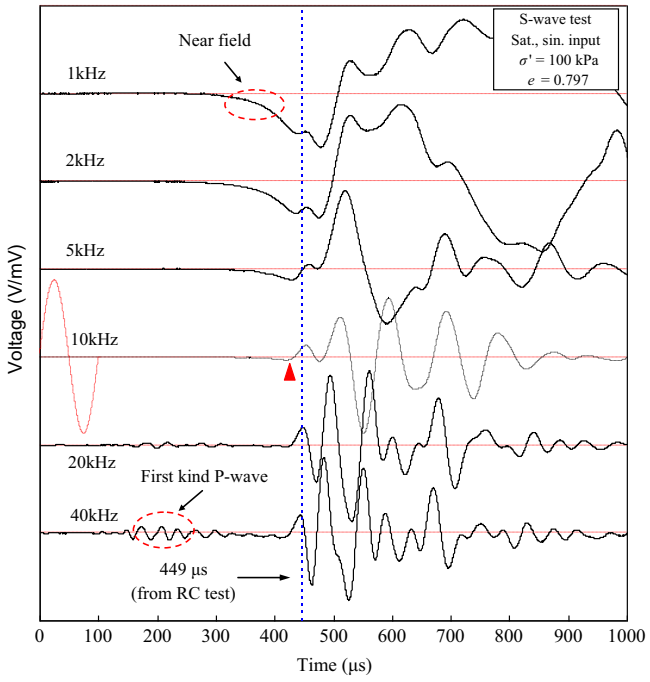

Fig. 12. Received S-wave signals in a saturated DT specimen.

arrival of the S-wave from the received signals, although the near field effect still exists, especially at low frequencies. Yamashita et al. (2009) have reported similar results, namely, that the scatter of G_0 is smaller under saturated conditions than under dry conditions. In addition, the signals in Fig. 12 confirm that the wave form corresponding to the first arrival has amplitude that is much smaller than that of the succeeding ones. At high input frequencies (e.g., 40 kHz), the first kind of P-wave (Biot, 1956) appears since the calculated wave velocity is near the P-wave velocity in water. It is noted that the travel time under saturated conditions obtained from the BE test is considerably smaller than that from the RC test. The reason is the dispersion of the S-wave in saturated soil, which will be illustrated in the following.

4.2. Dispersion of S-wave in saturated soil

Fig. 13 compares the G_0 values of saturated DT specimens at various densities and confining pressures obtained from BE, RC and TS tests. Note that the conventional saturated density, ρ_{sat}, was used to convert the measured V_s to G_0 in Eq. (2) and to calculate the I value in Eq. (3). It is seen that the G_0 values from the RC and TS tests agree well with each other and are consistent with the observation done under dry conditions. However, in contrast to the dry conditions, the G_0 values under saturated conditions obtained from BE tests are apparently larger than those obtained from RC and TS tests. The explanation lies in that the density involved in the S-wave propagation in the BE tests is less than the saturated density due to the relative movement between the solid and the fluid phases (Biot, 1956).

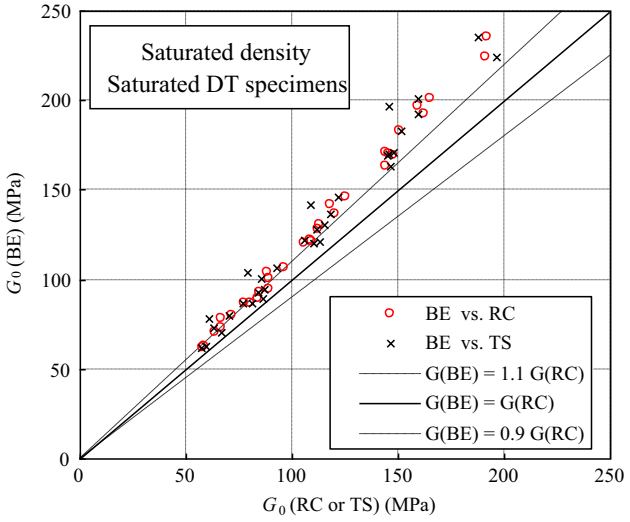

Fig. 13. Comparison of G_0 of saturated DT specimens obtained by BE, RC and TS tests with the saturated density.

Biot (1956) performed an excellent theoretical study on the wave propagation in saturated porous media and obtained S-wave velocity V_s as

$$V_s = \sqrt{\frac{G_0}{\frac{E_r + (E_r^2 + E_i^2)^{1/2}}{2}\rho_{sat}}} = \sqrt{\frac{G_0}{\xi\rho_{sat}}} = \sqrt{\frac{G_0}{\rho_{Biot}}} \quad (5)$$

where E_r and E_i are two dimensionless parameters, ρ_{Biot} is the effective (or actual) density involving the S-wave propagation, according to Biot's theory, and $\xi = \rho_{Biot}/\rho_{sat}$ is a density coefficient indicating the percentage of saturated density involving the S-wave propagation. The value for ξ quantifies the degree of coupling between the solid and the fluid phases (Yang and Sato, 1998), and depends on the properties of the soil and the wave frequency.

A typical dispersion curve of ξ for Toyoura sand is shown in Fig. 14, where f is the wave frequency and f_c is the characteristic frequency which is evaluated by

$$f_c = \frac{ng}{2\pi k_h} \quad (6)$$

where n is the porosity of the soil, $g = 9.81$ (m/s^2) is the gravity acceleration and k_h is the hydraulic conductivity (in m/s). The k_h value for Toyoura sand is evaluated by the Kozeny–Carman equation with reference value $k_h = 1.45 \times 10^{-4}$ m/s at the void ratio of 0.617 (Kamon et al., 2004).

If the wave frequency is low ($f < 0.1 f_c$), ξ becomes unity, indicating that the solid and the fluid phases can be treated as fully coupled and move together in the S-wave propagation. If the wave frequency is high ($f >> f_c$), however, the viscous coupling can be ignored and ξ can be expressed as

$$\xi = 1 - \frac{n\rho_f}{\tau[(1-n)\rho_s + n\rho_f]} \quad (7)$$

where ρ_s is the density of the solid particles, ρ_f is the density of the fluid and τ is the tortuosity factor of the pore space

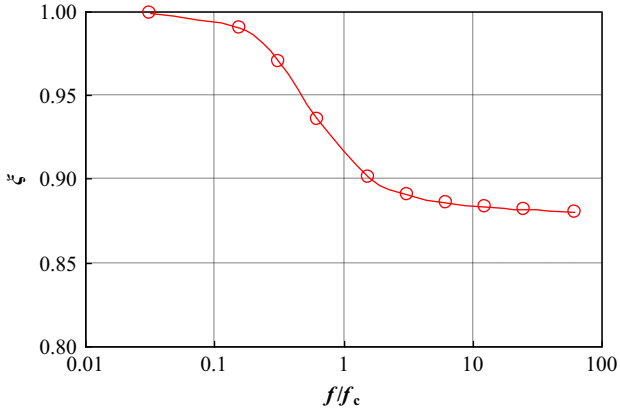

Fig. 14. Dispersion curve of the density coefficient for Toyoura sand.

representing the inertial coupling. The value of τ is difficult to determine; here it is calculated approximately by $\tau = (1+n)/2n$ (Youn et al., 2008; Biot, 1956).

Table 2 lists the typical values for f_c and ξ at different void ratios. For the tested void ratio of 0.86–0.70 (or relative density 30–80%) f_c is in the range of 2.1–3.2 kHz. The resonant frequencies in the RC tests are generally between 50–90 Hz, and therefore, are located in the low frequency range. Hence, the saturated density should be used to calculate the I value of the saturated specimen. However, the wave frequency in the BE tests is in the high frequency range; and thus, the density which accounts for the wave dispersion effect should be adopted for the evaluation of G_0 in Eq. (2).

Fig. 15 compares the G_0 values of the saturated DT specimens obtained from the BE tests using ρ_{Biot} in Eq. (2), along with those from the RC tests using ρ_{sat} and from the TS tests. As seen in Fig. 15, the G_0 values from the BE tests, using ρ_{Biot} in Eq. (2), are reasonably consistent with those from the RC and TS tests, indicating that relative movement exists between the solid and the fluid phases. The results here illustrate the importance of accounting for the frequency effect in evaluating G_0 in saturated soil using BE tests. The results also explain that, according to the observations by Yamashita et al. (2007) (refer to Figs. 4.58 and 4.59 in that paper), BE tests yield similar G_0 values under dry conditions, but considerably higher values under saturated conditions in comparison to RC, TS and triaxial tests.

It should be emphasized that S-wave velocity V_s in Eq. (1) from the RC tests is an "assumed" velocity, in contrast to the direct measurement in Eq. (4) from the BE tests. In the RC tests, the resonant frequency is directly measured and the V_s is

Table 2
Characteristic frequencies and density coefficients for Toyoura sand at different void ratios.

e	n	f_c (kHz)	τ	ξ[a]
0.700	0.412	3.19	1.714	0.89
0.800	0.444	2.44	1.625	0.87
0.860	0.462	2.11	1.581	0.86

[a]Based on the wave frequency of 10 kHz.

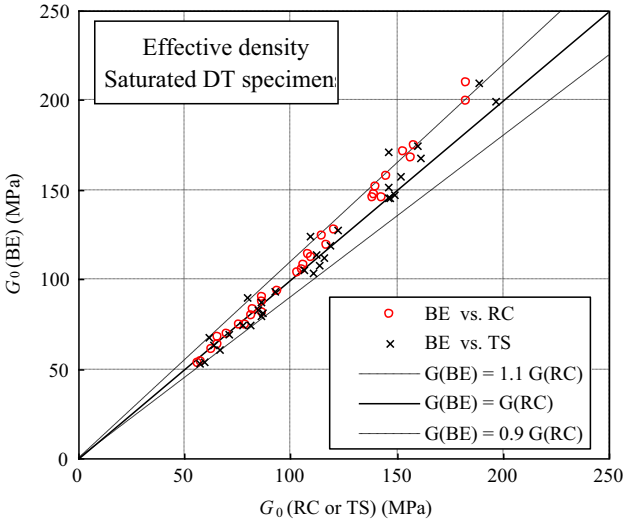

Fig. 15. Comparison of G_0 values of saturated DT specimens obtained by BE, RC and TS tests with Biot's effective density.

back calculated based on Eqs. (2) and (3), where an "assumed" density is usually used to calculate the I value. Then, the G_0 value is determined based on the calculated V_s and the "assumed" density. The "assumption" of different values for mass density (i.e., ρ_{sat} or ρ_{Biot}) has little effect on the calculated G_0, although it has an apparent effect on the calculated V_s. The mechanism is that the effect of density on G_0 is canceled when I/I_0 is small, which is the usual case in RC tests. When I/I_0 is small, by combining Eqs. (1)–(3), G_0 can be given as

$$G_0 = \rho\left(\frac{2\pi f_n L}{\beta}\right)^2 = \frac{(2\pi f_n)^2 L I_0}{J} \tag{8}$$

where J is the polar moment of inertia of the cross-section of the specimen and is related to I by $I=\rho JL$. Evidently, the value of G_0 is independent of the density. In other words, RC tests always correctly measure the G_0 value of the specimen, although the V_s value depends on the "assumed" density. On the other hand, the G_0 value in BE tests depends on the "assumed" density, as indicated by Eq. (2). Qiu and Fox (2008) performed a parametric study to evaluate the actual mass density in wave propagation at different frequencies for different types of soil. They used the data in RC tests by Hardin and Richart (1963) to illustrate the need to account for the wave dispersion under saturated conditions, but, as discussed above, the correction does not appear to be appropriate for RC tests.

Moreover, it is widely recognized that the saturation condition has no effect on small strain shear modulus G_0 as the water has no shear resistance. To check this issue and for a better comparison, a general empirical equation for sand (Hardin and Richart, 1963) is used here to analyze the G_0 values to account for the difference in void ratio and confining pressure between the tested specimens:

$$G_0 = AF(e)\left(\frac{\sigma'}{p_a}\right)^n \tag{9}$$

where A is a constant reflecting the soil properties and the fabric, σ' is the effective confining pressure (in kPa), p_a is a reference stress of 98 kPa, n is a stress exponent and $F(e)$ is a void ratio function reflecting the effect of the packing density. Here, $F(e)=(2.17-e)^2/(1+e)$ is adopted (Iwasaki and Tatsuoka, 1977). Note that the G_0 values in Eq. (9) are in MPa.

Table 1 lists the fitting results for the test data. The G_0 value of Toyoura sand under saturated conditions is about 7–10% less than that under dry conditions for all the test methods. This finding is consistent with the results of RC tests by Tatsuoka et al. (1979) and BE tests by Nakagawa et al. (1997). The possible explanation is that weak layers are formed on particle surfaces under saturated conditions, thus decreasing the contact stiffness to some extent (Nakagawa et al., 1997).

5. Effect of sample preparation method

To study the potential effect of the sample preparation method (SPM), the G_0 values of sand specimens reconstituted by the DT, AP and MT methods at 100 kPa are compared in Fig. 16. Note that all the specimens were tested under saturated conditions so as to eliminate the capillary effect in the MT specimens and that Biot's effective density, accounting for the wave dispersion, was adopted in the analysis of the BE test data. For MT specimens, the G_0 values from BE tests are apparently higher than those from RC and TS tests. On the other hand, for DT and AP specimens, the BE, RC and TS tests provide similar G_0 values. To quantify the effect of SPM, the G_0 values of these specimens are fitted by Eq. (9) and the results are listed in Table 1. As seen in Table 1, the G_0 values for DT and AP specimens from the BE, RC and TS tests are consistent with each other, indicating the negligible effect of the test method. However, for MT specimens, BE tests provide apparently (about 14%) higher G_0 values than RC tests on identical specimens, while TS tests provide similar results to RC tests.

From the BE tests, the G_0 values of the MT specimens are around 17–21% higher than those of the AP and DT specimens; however, from the RC and TS tests, the G_0 values of the MT specimens are around 6–7% higher than those of the AP and DT specimens. These results indicate the coupled effect of SPM and the test method. They also explain the discrepancies regarding the effect of SPM on G_0 in literature. For example, Tatsuoka et al. (1979), based on RC tests, reported that the SPM had a negligible effect, while De Alba et al. (1984), based on BE tests, showed that the G_0 values of MT specimens were around 20% higher than those of AP specimens. Gu and Yang (2011) have further suggested that this coupled effect depends on the soil type, by showing that G_0 values of well-graded completely decomposed granite specimens prepared by the MT method from BE tests were around 50% higher than those from RC tests.

The coupled effects of the test method and SPM can be conceptually explained by the following two aspects. The first one is that BE tests measure the "local" stiffness of the specimen (i.e., the stiffness along the wave travel path), while RC and TS tests measure the average or the "global" stiffness of the whole specimen. The second aspect is related to the difference in compaction energy between different SPM.

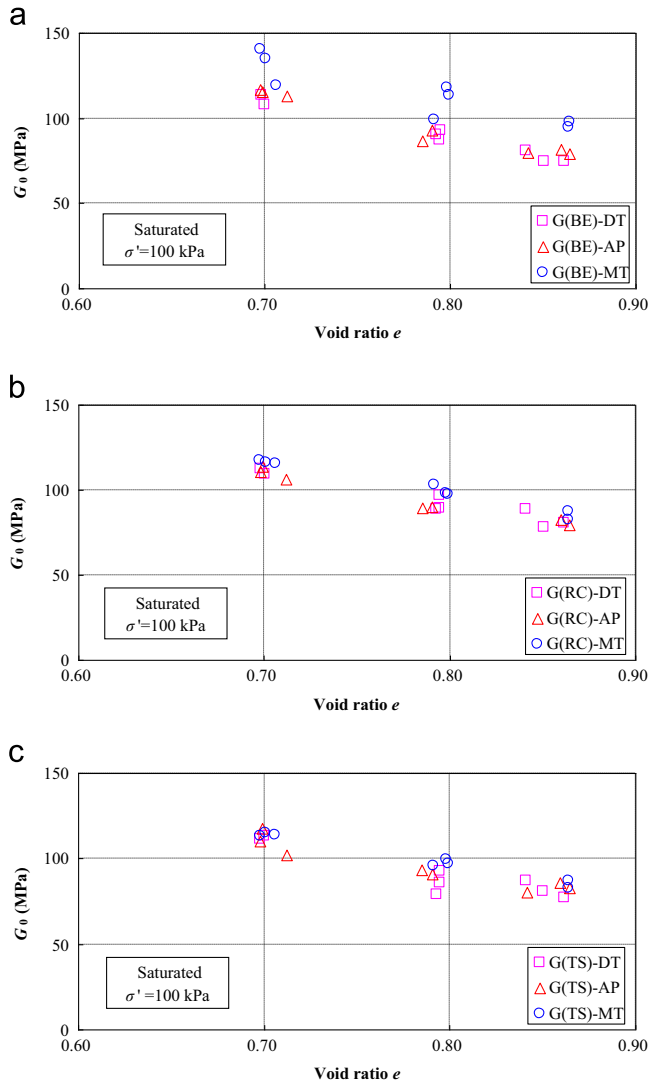

Fig. 16. G_0 values of specimens prepared by different methods obtained by (a) BE, (b) RC and (c) TS tests at 100 kPa.

Compared with the DT and AP methods, the MT method requires much more compaction energy to achieve the same void ratio due to the induced capillary force occurring in the moist state. Frost and Park (2003) showed that the average compaction peak stress in the MT method was around 75 kPa at $D_r=50\%$ and 150 kPa at $D_r=75\%$ for Ottawa sand with $D_{50}=0.35$ mm. Therefore, it is reasonable to deduce that the stress history in the MT method decreases the possibility of the existence of local voids and increases the number of contacts (Gu and Yang, 2013), resulting in a more stable structure and an increase in stiffness. Moreover, the wave propagation path (or the force chain) is enhanced during the compaction, which results in the "local" stiffness increasing more significantly than the "global" one.

6. Summary and conclusions

In this study, a series of BE, RC and TS tests has been performed on Toyoura sand specimens at various effective confining pressures and densities under both dry and saturated conditions. The effects of the test method, the saturation and the sample preparation method on the G_0 values have been investigated in detail. The main results of the study are summarized as follows:

(1) The discrepancies in the G_0 values obtained from the different interpretation methods in the BE tests are mainly associated with the differences in frequency component and wave form between the input and output signals. The start–start method, with a proper identification of the first arrival, generally provides stable and reliable results compared to the other methods. Since the output signal usually has multiple cycles and the amplitude of the first cycle is usually not the largest one, the cross correlation method and the cross power method tend to yield much lower G_0 values than the start–start method.

(2) The dispersion of the S-wave appears to exist in saturated specimens in the BE tests and it mainly depends on the permeability of the soil. If dispersion exists, it is essential to use the effective density, rather than the saturated density, to convert the measured V_s to G_0 to account for the coupling between the solid and the fluid phases under saturated conditions. Otherwise, the G_0 value under saturated conditions from the BE tests may be over-estimated. The G_0 value from the RC tests does not depend on the density used (effective density or saturated density), but the indirectly measured S-wave velocity does.

(3) The G_0 values of the DT specimens from the BE, RC and TS tests are consistent with each other under both dry and saturated conditions as long as the effective density is used in the BE tests. The G_0 value under saturated conditions is about 7–10% lower than that under dry conditions.

(4) There is a coupled effect of the sample preparation method and the test method on the G_0 values of sand. For specimens prepared by the DT and AP methods, the G_0 values obtained from the BE, RC and TS tests are consistent with each other. However, for specimens prepared by the MT method, the G_0 values from the BE tests are around 14% higher than those from the RC and TS tests, and the G_0 values from the RC and TS tests agree well with each other. On the other hand, the G_0 values of the MT specimens from the BE tests are around 17–21% higher than those of the AP and DT specimens, but the G_0 values of the MT specimens from the RC and TS tests are only around 6–7% higher than those of the AP and DT specimens. This coupled effect is probably due to the difference in compaction energy used in these sample preparation methods and the difference in the principles involved in these test methods (i.e., BE tests measure the local stiffness of a specimen, whereas RC and TS tests measure the global stiffness of the specimen).

Acknowledgments

The authors wish to acknowledge the support provided by the National Natural Science Foundation of China (Nos.

51428901 and 51308408) and by the National Basic Research Program of China (No. 2012CB719803). The various types of support provided by The University of Hong Kong during the course of this research are also gratefully acknowledged.

References

Andrus, R.D., Stokoe, K.H.I.I., 2000. Liquefaction resistance of soils from shear-wave velocity. J. Geotech. Geoenviron. Eng. 126 (11), 1015–1025.

Biot, M.A., 1956. Theory of propagation of elastic waves in a fluid-saturated porous solid. I. Low frequency range & II. Higher frequency range. J. Acoust. Soc. Am. 28 (2), 168–191.

Brignoli, E.G.M., Gotti, M., Stokoe, K.H.I.I., 1996. Measurement of shear waves in laboratory specimens by means of piezoelectric transducers. Geotech. Test. J. 19 (4), 384–397.

Camacho-Tauta, J., Sanrtos, J.A., Viana da Fonseca, A., 2014. Two-bender receivers frequency domain analysis in resonant-column tests. Advances in Soil Dynamics and Foundation Engineering ASCE-GSP, vol. 240, pp. 72–82.

De Alba, P., Baldwin, K., Janoo, V., Roe, G., Celikkol, B., 1984. Elastic-wave velocities and liquefaction potential. Geotechn. Test. J. 7 (2), 77–87.

Dyvik, R., Madshus, C., 1985. Lab measurements of G_{max} using bender element. In: Khosla, V. (Ed.), Advances in the Art of Testing Soils under Cyclic Conditions. ASCE, New York, pp. 186–196.

Ezaoui, A., Di Benedetto, H., 2009. Experimental measurements of the global anisotropic elastic behavior of dry Hostun sand during triaxial tests, and the effect of sample preparation. Géotechnique 59 (7), 621–635.

Ferreira, C., Viana da Fonseca, A., Santos, J.A., 2006. Comparison of simultaneous bender elements and resonant-column tests on Porto residual soil. Soil Stress–strain Behavior: Measurement, Modeling and Analysis, Geotechnical Symposium in Roma, pp. 523–535.

Frost, J.D., Park, J.-Y., 2003. A critical assessment of the moist tamping technique. Geotech. Test. J. 26 (1), 55–70.

Greening, P.D., Nash, D.F.T., 2004. Frequency domain determination of G_0 using bender elements. Geotech. Test. J. 27 (3), 288–294.

Gu, X.Q., 2012. Dynamic properties of granular materials at the macro and micro scales (PhD thesis). The University of Hong Kong, Hong Kong.

Gu, X.Q., Yang, J., 2011. Laboratory measurement of small strain shear modulus of completely decomposed granite. In: Proceedings of the 15th European Conference on Soil Mechanics and Geotechnical Engineering, Athens, Greece.

Gu, X.Q., Yang, J., 2013. A discrete element analysis of elastic properties of granular materials. Granul. Matter 15 (2), 139–148.

Gu, X.Q., Yang, J., Huang, M.S., 2013. Laboratory measurements of small strain properties of dry sands by bender element. Soils Found. 53 (5), 735–745.

Hardin, B.O., Richart, F.E., 1963. Elastic wave velocities in granular soils. J. Soil Mech. Found. Div. 89 (SM1), 39–56.

Hoque, E., Tatsuoka, F., 1998. Anisotropy in elastic deformation of granular materials. Soils Found. 38 (11), 163–179.

Iwasaki, T., Tatsuoka, F., 1977. Effect of grain size and grading on dynamic shear moduli of sand. Soils Found. 17 (3), 19–35.

Kamon, M., Endo, K., Kawabata, J., Inui, T., Katsumi, T., 2004. Two-dimensional DNAPL migration affected by groundwater flow in unconfined aquifer. J. Hazard. Mater. 110 (1), 1–12.

Kim, D.S., Stokoe, K.H., Roesset, J.M., 1991. Characterization of material damping of soils using resonant column and torsional shear tests. In: Proceedings of 5th International Conference on Soil Dynamics and Earthquake Engineering, Karlsruhe, Germany.

Kokusho, T., 1980. Cyclic triaxial test of dynamic soil properties for wide strain range. Soils Found. 20 (2), 45–60.

Lee, J.-S., Santamarina, J.C., 2005. Bender element, performance and signal interpretation. J. Geotech. Geoenviron. Eng. 131 (9), 1063–1070.

Lings, M.L., Greening, P.D., 2001. A novel bender/extender element for soil testing. Géotechnique 51 (8), 713–717.

Nakagawa, K., Soga, K., Mitchell, J.K., 1997. Observation of Biot compressional wave of the second kind in granular soils. Géotechnique 47 (1), 133–147.

Qiu, T., Fox, P.J., 2008. Effective soil density for propagation of small strain shear waves in saturated soil. J. Geotech. Geoenviron. Eng. 134 (12), 1815–1819.

Rashidian, M., Ishihara, K., Kokusho, T., Kanatani, M., Okamoto, T., 1995. Effect of sample preparation methods on shear wave velocity. In: Proceedings of the Second International Conference on Seismology and Earthquake Engineering, Teheran, Iran, pp. 1501–1508.

Richart, F.E., Hall, J.R., Woods, R.D., 1970. Vibrations of Soils and Foundations. Prentice-Hall, Englewood Cliffs, New Jersey.

Shirley, D.J., Hampton, L.D., 1978. Shear-wave measurements in laboratory sediments. J. Acoust. Soc. Am. 63 (2), 607–613.

Souto, A., Hartikainen, J., Ozudogru, K., 1994. Measurement of dynamic parameters of road pavement materials by the bender element and resonant column tests. Géotechnique 44 (3), 519–526.

Stokoe, K.H.II, Hwang, S.K., Lee, J.N.-K., 1995. Effects of various parameters on the stiffness and damping of soils at small to medium strains. In: Proceedings of the First International Conference on Prefailure Deformation Characteristics of Geomaterials, vol. II, pp. 785–816.

Sze, H.Y., Yang, J., 2014. Failure modes of sand in undrained cyclic loading: impact of sample preparation. J. Geotech. Geoenviron. Eng. ASCE, 140; 152–169.

Tatsuoka, F., Iwasaki, T., Yoshida, S., Fukushima, S., Sudo, H., 1979. Shear modulus and damping by drained tests on clean sand specimens reconstituted by various methods. Soils Found. 19 (1), 39–54.

Viana da Fonseca, A., Ferreira, C., Fahey, M., 2009. A framework interpreting bender element tests, combining time-domain and frequency-domain methods. Geotech. Test. J. 32 (2), 1–17.

Viggiani, G., Atkinson, J.H., 1995. Interpretation of bender element tests. Géotechnique 45 (1), 149–154.

Yamashita, S., Fujiwara, T., Kawaguchi, T., Mikami, T., Nakata, Y., Shibuya, S., 2007. International parallel test on the measurement of G_{max} using bender elements organized by TC-29. ISSMGE TC-29 Report, pp. 1–76.

Yamashita, S., Kawaguchi, T., Nakata, Y., Mikami, T., Fujiwara, T., Shibuya, S., 2009. Interpretation of international parallel test on the measurement of G_{max} using bender elements. Soils Found. 49 (4), 631–650.

Yang, J., Gu, X.Q., 2013. Shear stiffness of granular material at small strain: does it depend on grain size?. Géotechnique 63 (2), 165–179.

Yang, J., Sato, T., 1998. Influence of viscous coupling on seismic reflection and transmission in saturated porous media. Bull. Seismol. Soc. Am. 88 (5), 1289–1299.

Yang, J., Yan, X.R., 2009. Factors affecting site response to multi-directional earthquake loading. Eng. Geol. 107, 77–87.

Youn, J.-U., Choo, Y.-W., Kim, D.-S., 2008. Measurement of small-strain shear modulus G_{max} of dry and saturated sands by bender element, resonant column, and torsional shear tests. Can. Geotech. J. 45, 1426–1438.